Journal of Drug Delivery Science and Technology 44 (2018) 467–474

Contents lists available at ScienceDirect

Journal of Drug Delivery Science and Technology

journal homepage: www.elsevier.com/locate/jddst

Fabrication and *in vitro* evaluation of magnetic PLGA nanoparticles as a potential Methotrexate delivery system for breast cancer

Molood Alsadat Vakilinezhad[a,b], Shohreh Alipour[b], Hashem Montaseri[b,*]

[a] Department of Pharmaceutics, Faculty of Pharmacy, Tehran University of Medical Sciences, Tehran, Iran
[b] Department of Quality Control, Faculty of Pharmacy, Shiraz University of Medical Sciences, Shiraz, Iran

ARTICLE INFO

Keywords:
Methotrexate
PLGA
Localized drug delivery systems
Magnetic drug delivery systems

ABSTRACT

Polymeric magnetic nanoparticles due to their ability in overcoming drug retention in targeted organs have been noticed for localized drug delivery. Methotrexate (MTX) is one of the most frequently used chemotherapeutic agent and disease modifying anti-rheumatic drug with high hydrophilicity feature which leads to its rapid clearance even in local injections. The aim of this study is to prepare and evaluate MTX-loaded PLGA magnetic nanoparticles (MPNPs) to overcome these obstacles. MPNPs were prepared using double emulsion-solvent evaporation method and characterized. The particles size, morphology, magnetization saturation, drug and magnetite encapsulation efficiency, MTX release pattern from particles and cytotoxicity were evaluated. Using different drug to polymer ratio, PVA concentration and stirring speed, the minimum particle size of 390 nm was acquired. Approximately, 94.57% drug encapsulation efficiency resulted by further optimization. These particles have magnetization saturation of about 43emu/g with no remanence time and showed similar cell cytotoxicity in comparison with MTX solution. Considering the appropriate in vitro properties of selected MPNPs for magnetically guided drug targeting, it seems that promising results in reducing MTX side effects maybe expectable in further in vivo studies.

1. Introduction

The role of polymeric nanoparticles in biomedical fields could not be denied. Their small size, large surface area, and ability to controlled drug delivery have made them a potential therapeutic platform, especially in chemotherapeutical field [1,2]. However, neither chemotherapeutical agents nor polymeric carriers have specific tendency toward the cancerous site. Hence, their targeting ability is limited. Various strategies have been developed to overcome such limitation. Magnetically guided systems which consist of coupling polymeric carriers with magnetic nanoparticles can be mentioned, for instance [3].

Magnetic nanoparticles (MNPs) are remarkably attractive due to their application as contrast enhancement agents, as controlled drug delivery carriers, and in theranostics, hyperthermia treatment, and magnetofection [4]. In a magnetically guided drug delivery system, an external magnetic field is generally used to guide the injected magnetic carriers to the target site. The carriers stay at the target site and release their active substance until the end of therapy; and then, they are removed. Particles become magnetically active in the presence of an external magnetic field and revert to their de-active form as the external field is removed. This method is known as “magnetic drug delivery” [5–7].

Several studies have proved the benefits of magnetic drug carriers in diagnosing, monitoring, and treating cancer [1]. Magnetic drug carriers not only produce high local drug concentration and avoid the toxicity of other organs, but they can also keep drug away from the reticuloendothelial system [8,9].

Biocompatible magnetite particles, Fe_3O_4, have been widely investigated in the biological field. The most commonly used method to synthesize these particles is the co-precipitation technique [10]. Magnetic nano-sized particles have large surface energy, which leads to their aggregation. Besides, these bare metal particles are highly susceptible to oxidization, which may reduce their magnetism. Hence, coating is a proper method of stabilizing and protecting the bare magnetite particles [10]. However, it is noteworthy that coated stabilizers and protectants may create a magnetically dead layer on the surface of particles, which may reduce their magnetic properties [7]. Different coating materials have been investigated previously. For our interest, oleic acid was chosen as a coating agent as it preserves the magnetic properties of particles, resisting their precipitation and retaining their large magnetic moment [4].

* Corresponding author. Department of quality control, Faculty of Pharmacy, Shiraz University of Medical Sciences, Shiraz, Fars, Iran.
E-mail addresses: Moloodvakili@gmail.com (M.A. Vakilinezhad), Alipour_sh@sums.ac.ir (S. Alipour), Hmontase@sums.ac.ir (H. Montaseri).

https://doi.org/10.1016/j.jddst.2018.01.002
Received 21 October 2017; Received in revised form 30 December 2017; Accepted 3 January 2018
Available online 05 February 2018
1773-2247/

The pharmaceutical characteristics, as well as the biological safety and efficacy, of novel drug delivery systems are highly dependent on carrier properties [6]. Although natural polymers are less immunogenic, their different chemical composition is still a problem in pharmaceutical studies. Synthetic polymers, on the other hand, have specific components leading to predictable particle characteristics. Another advantage is that they can be synthesized with particular properties for desired applications. Among synthetic polymers Poly (lactic-co-glycolic acid), PLGA, is approved by FDA for therapeutic uses due to its biodegradability, biocompatibility and non-immunogenicity [11,12].

Methotrexate (MTX) is one of the most frequently used disease-modifying antirheumatic drugs (DMARD). It is also used as a folate antimetabolite chemotherapeutic agent [13,14]. MTX has some serious adverse effects including hepatic fibrosis, cirrhosis, and bone marrow suppression; this has impacted its notable benefits as a chemotherapy agent. Various microparticles and nanoparticles were investigated to overcome the difficulties of MTX administration in addition to increasing its retention time in the body and improving its bioavailability, half-life, and stability [14–17].

The encapsulation of hydrophilic drugs into hydrophobic carriers seems to be useful in creating a controlled release system [18]. Accordingly, this study hypothesized that MTX loaded PLGA particles containing magnetite nanoparticles, can show proper magnetic properties for targeted delivery in addition to preserving a controlled release system of loaded MTX.

These particles should present some specificity including high magnetic properties to enable magnetic guidance within the vasculature; appropriate size to avoid rapid excretion and/or capillary occlusion; and the ability to carry a proper amount of drug, preserve its bioactivity, and release it in a controlled manner [5,9].

Generally, this investigation intended to prepare a magnetically guided system for MTX delivery. Therefore, the objectives of this study were to prepare MTX loaded PLGA particles containing oleic acid coated magnetite, taking into consideration proper MTX loading and cytotoxicity on the tumoric cell line.

Table 1
Impact of drug to polymer ratio, PVA concentration and stirring speed on MPNPs size.

Formulation	Drug:Polymer	PVA%	Stirring speed (rpm)	Particle Size(μm) ± SPAN
MPNP-1	1:1	1	750	0.42 ± 1.05
MPNP-2	1:1	1	1000	0.39 ± 0.91
MPNP-3	1:1	1	1400	0.45 ± 1.05
MPNP-4	1:1	2	750	0.76 ± 1.36
MPNP-5	1:1	2	1000	0.45 ± 0.98
MPNP-6	1:1	2	1400	1.26 ± 1.71
MPNP-7	1:1	3	750	1.89 ± 2.00
MPNP-8	1:1	3	1000	0.54 ± 0.86
MPNP-9	1:1	3	1400	1.99 ± 1.97
MPNP-10	1:2	1	750	1.07 ± 2.59
MPNP-11	1:2	1	1000	0.60 ± 1.45
MPNP-12	1:2	1	1400	0.84 ± 1.65
MPNP-13	1:2	2	750	0.75 ± 1.21
MPNP-14	1:2	2	1000	0.61 ± 1.77
MPNP-15	1:2	2	1400	0.91 ± 1.47
MPNP-16	1:2	3	750	23.39 ± 1.43
MPNP-17	1:2	3	1000	0.66 ± 1.21
MPNP-18	1:2	3	1400	1.53 ± 2.19
MPNP-19	1:4	1	750	0.86 ± 1.83
MPNP-20	1:4	1	1000	0.72 ± 0.82
MPNP-21	1:4	1	1400	1.15 ± 1.56
MPNP-22	1:4	2	750	34.22 ± 1.67
MPNP-23	1:4	2	1000	6.10 ± 0.47
MPNP-24	1:4	2	1400	555.23 ± 0.53
MPNP-25	1:4	3	750	105.82 ± 1.16
MPNP-26	1:4	3	1000	569.05 ± 0.53
MPNP-27	1:4	3	1400	797.002 ± 0.39

2. Materials and methods

2.1. Materials

Iron (II) chloride tetrahydrate, Iron (III) chloride hexahydrate, Ammonium hydroxide, oleic acid, and Span®80 were provided in analytical grade from Merck, Germany. Methotrexate was purchased from EBEWE, Austria. Polyvinyl alcohol (MW ~ 72000; 97.5–99.5mol% hydrolysis) was provided from Fluka, Switzerland; and PLGA Resomer® RG502H (Carboxylate end group) was procured from Boehringer Ingelheim, Germany. Cell lines were received from Pasteur institute, Iran; and essential cell culture media components, RPMI 1640, fetal bovine serum (FBS) and Penicillin-streptomycin provided from Biosera, Ringmer, UK. 3-(4,5-Dimethylthiazol-2-yl)-2,5-diphenyltetrazolium bromide, MTT, was purchased from Sigma, USA.

2.2. Preparation and size optimization of MPNPs

Oleic acid coated magnetite nanoparticles (OMNPs) were synthesized using co-precipitation method previously published in fair detail by Montaseri et al. [4]. Briefly, aqueous iron salts of $FeCl_3$ and $FeCl_2$, were prepared in deoxygenated water. The media were heated up to 70 ± 5 °C and mixed using probe sonicator (Hielscher, Germany). Magnetite crystals were formed upon pH change induced by addition of ammonium hydroxide alkaline solution under nitrogen purge. Oleic acid was then added dropwise to stabilize the primary magnetite particles. OMNPs were separated and washed using magnetic decantation.

MTX loaded PLGA magnetic nanoparticles (MPNPs) were prepared by double emulsion solvent evaporation technique [18,19]. Drug to polymer ratio and PVA concentration were selected as independent factor (Table 1). The specific amount of MTX solution (as a primary water phase, W_1) was emulsified with synthesized OMNPs (200 μl, 1% w/v) and the various amount of PLGA dissolved in 2 ml dichloromethane (as an oil phase, O), by 10 s sonication at 100 W amplitude using probe sonicator (Hielscher, Germany). This primary emulsion (W_1/O) was added to the 5 ml polyvinyl alcohol (PVA) surfactant solution in three different concentrations (1, 2 or 3%w/v) and was sonicated for 1 min. The final $W_1/O/W_2$ emulsion was added to the water extraction media slowly and magnetically stirred at three different speed (750, 1000 or 1400 rpm) for 4 h at room temperature. The resulted particles were centrifuged for 20 min, washed 3 times with distilled water, freeze-dried and stored at 4 °C.

The effects of different drug to polymer ratio, PVA concentration and solvent evaporation speed were investigated as full factorial design. All formulations prepared in triplet in which number-based median sizes were measured.

2.3. Optimization of MTX encapsulation efficiency and loading

The smallest sized nanoparticle in each category was selected to determine MTX loading (Table 2). To optimize the MTX encapsulation efficiency four different factors including drug amount (drug to polymer ratio: 1, 2.5, 5), stabilizer effect to stabilize primary emulsion and reduce MTX escape from the internal phase (0, 2, 4%v/v span®80), extraction water phase pH (5, 7, 9) and extraction phase component (water, PVA1%, paraffin1%) were evaluated (Table 3).

2.4. Characterization of MPNPs

2.4.1. Size, zeta potential and morphology of MPNPs

Acquired particles size was evaluated in respect of number-based diameter using laser diffraction technique (Shimadzu SALD- 2101, Japan). The zeta potential of the selected MPNPs were measured using NANO-flex®, USA. Morphology of the selected MPNPs was studied using scanning electron microscopy (SEM) (Cambridge, S-360, U.K.). Samples were gold coated by sputter coater (Fisons, model 7640, UK) prior to

Table 2
MTX encapsulation efficiency and drug loading of selected MPNPs.

Formulation	MPNP-2	MPNP-5	MPNP-8	MPNP-11	MPNP-14	MPNP-17	MPNP-20
%EE	6.13 ± 2.6	7.26 ± 2.9	8.28 ± 3.7	2.09 ± 0.5	2.39 ± 0.6	4.78 ± 1.6	3.51 ± 0.4
%DL	0.56 ± 0.2	0.66 ± 0.3	0.75 ± 0.3	0.1 ± 0.23	0.11 ± 0.3	0.23 ± 0.1	0.08 ± 1.3

the image capturing.

2.4.2. Evaluation of magnetite loading in MPNPs

Iron content of MPNPs was measured using atomic absorption method (Perkin Elmer Precisely, USA) in wavelength of 248 nm. Briefly 2 mg of MPNPs were dissolved in nitric acid (2 M). The iron concentration was measured using the previously validated standard curve in a range of 1–4 μg/ml.

2.4.3. Magnetic properties of MPNPs

Alternating Field Gradient Magnetometer (AFGM-MDK, Iran) was used to evaluate the magnetic properties of selected MPNPs. Magnetization curve of fixed sample between the pole pieces was obtained in Magnetic field of −10000 Oe to +10000 Oe [4].

2.4.4. Fourier transform infra-red spectroscopy (FTIR)

Possible interactions between polymer and/or drug and/or OMNP were investigated using FTIR spectroscopy (VERTEX70 spectrophotometer, Bruker®, Germany). Spectra were taken in range of 400–4000 cm^{-1} [4].

2.4.5. Determination of MTX in MPNPs

To determine the encapsulated amount of MTX in nanoparticles, MPNPs were dissolved in dichloromethane and water was added to extract MTX. The dissolved polymer was precipitated by evaporating dichloromethane phase using nitrogen purge. The mixture was centrifuged at 5000 rpm for 10 min and the clear supernatant was used to measure MTX concentration. Loading parameters were calculated using the following formulas:

$$\%Drug\ Loading\ (\%DL) = \frac{Amount\ of\ drug\ in\ particles}{weight\ of\ particles} \times 100$$

$$\%Encapsulation\ Efficiency\ (\%EE) = \frac{Practical\ drug\ loading}{Theoretical\ drug\ loading} \times 100$$

MTX assay performed by HPLC system (Waters, model600, USA) equipped with analytical column of ODS-3 (250 × 4.6 mm). The mobile phase was phosphate-citrate buffer: acetonitrile (75:25 v/v), adjusted to pH of 3 with acetic acid. Mobile phase pumped at flow rate of 0.8 ml/min. The UV detector's wavelength set to 307 nm. All assays were done in triplicate.

2.4.6. In vitro release of MTX

MTX *in vitro* release from MPNPs was experimented in phosphate buffer solution, PBS, (pH 7.4) [20,21]. 2 mg of each formulation was suspended in 5 ml freshly prepared releasing media that was shaken vertically while incubated in 37 °C (JAL Tajhiz lab tech, JTSL 20, Iran). Samples were removed at 15 and 30 min and 1, 2, 4, 6, 8, 24, 48 and 72 h and were centrifuged at 5500 rpm for 10 min. Supernatant's solution was used to determine the MTX concentration. All experiments were performed in triplicate. Percentage of drug release was calculated using following formula:

$$\%Drug\ Release = \frac{Amount\ of\ drug\ at\ each\ time\ point}{Quantity\ of\ drug\ loaded} \times 100$$

The *in vitro* drug release data were plotted in four models of zero-order, first-order, Higuchi and Korsmeyer-Peppas. The acquired linear regressions were determined the best model fitted [12].

2.4.7. In vitro cytotoxicity study

MTT cell viability assay was performed on human mammary gland epithelial cell of breast adenocarcinoma, i.e. SK-BR-3 cell line. Cells were cultivated in medium of RPMI with 10% FBS and 1% penicillin-streptomycin at 37 °C in humidified environment consists of 5% CO_2. Cells were seeded in 96-well plates at concentration of 5000 cells per well. The 48 h incubation allows cell attachment. Cells were then incubated with MTX, OMNPs, blank PLGA magnetic nanoparticles and selected MPNPs for 24, 48 and 72 h. At these times, media containing MTT (5 mg/ml) replaced the formulations and cells were incubated for 4 h. Afterward, MTT was removed and DMSO was added to lyse cells. Absorptions were read by Microplate reader at 492 nm. Untreated control cells assumed to have 100% viability [22].

2.5. Data analysis and statistics

The data were reported as mean ± SD unless mentioned otherwise. For statistical analysis, ANOVA test with the Tukey Post Hoc test were performed by SPSS® statistics 17.0 (windows based version). Statistical significant was considered to be p value < 0.05.

Table 3
Optimization of MTX encapsulation efficiency and loading.

Formulation	Drug: Polymer	Span®80 concentration (%)	pH of extraction phase	Extraction media	%EE	%DL
MPNP-8	1:1	-	-	-	8.28 ± 3.7	0.75 ± 0.3
MPNP-28	2.5:1	-	-	-	16.87 ± 5.1	3.37 ± 1.03
MPNP-29	5:1	-	-	-	13.07 ± 8.6	4.36 ± 2.9
MPNP-28	2.5:1	0	-	-	16.87 ± 5.1	3.37 ± 1.0
MPNP-30	2.5:1	2	-	-	33.24 ± 2.2	6.65 ± 4.4
MPNP-31	2.5:1	4	-	-	27.87 ± 5.5	5.57 ± 1.1
MPNP-32	2.5:1	2	5	-	76.44 ± 2.91	15.29 ± 4.5
MPNP-30	2.5:1	2	7	-	33.24 ± 2.2	6.65 ± 4.4
MPNP-33	2.5:1	2	9	-	5.09 ± 2.0	1.02 ± 0.4
MPNP-32	2.5:1	2	-	Water (pH = 5)	76.44 ± 2.91	15.29 ± 4.5
MPNP-34	2.5:1	2	-	PVA 1%	77.42 ± 1.8	15.48 ± 3.6
MPNP-35	2.5:1	2	-	Paraffin 1%	94.57 ± 2.06	18.91 ± 4.1

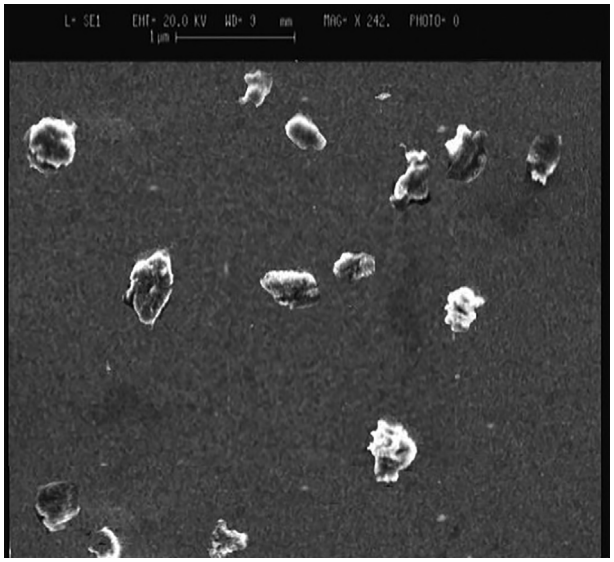

Fig. 1. SEM of MPNP-35. (bar size = 1 µm).

3. Results

3.1. Preparation and size optimization of MPNPs

The effect of drug to polymer ratio, PVA concentration and solvent evaporation speed on particle size were studied. Number-based diameters of acquired particles were varied widely in different preparation conditions (Table 1). The smallest particle size; i.e. 390 ± 0.91 nm, were produced using drug to polymer ratio of 1, PVA 1% and the stirring speed of 1000 rpm.

3.2. Optimization of MTX loading parameters

Loading parameters of the smallest nanometer sized particle of each category was evaluated (Table 2). The highest encapsulation efficiency of 8.28 ± 3.7% obtained for MPNP-8 formulation. Therefore, various modifications were conducted to elevate the encapsulation efficiency% of MTX. Finally, 94.57 ± 2.06% encapsulation efficiency and 18.91 ± 4.1% drug loading obtained in MPNP-35 formulation containing drug to polymer ratio of 2.5, stabilizing agent of primary emulsion (W_1/O) 2% (span®80) and extraction phase containing 1% liquid paraffin (Table 3).

3.3. Characterization of MPNPs

3.3.1. Size, zeta potential and morphology of MPNPs

The acquired particles sizes are reported in Table 1. The zeta potentials of −30.2, −31, −28.6 and −34.7 were obtained for MPNP-28, MPNP-30, MPNP-32 and MPNP-35 formulations, respectively.

As shows in Fig. 1, morphology of the selected nanoparticles, i.e. MPNP-35, were studied using SEM which showed almost uni-dispersed rock-like particles with approximate size of 400 nm.

3.3.2. Evaluation of magnetite loading in MPNPs

The amount of loaded magnetite was measured according to standard curve obtained by atomic absorption method (Fig. 2a). Results indicated that the 1%w/v OMNPs suspension contains 64.7 mg/ml iron ion and encapsulation efficacy of OMNPs in MPNP-35 was 84.31%.

3.3.3. Magnetic properties of MPNPs

Fig. 2 depicted magnetization curve of OMNP and MPNP-35. The magnetic saturation was 72emu/g and 43emu/g, respectively.

3.3.4. Fourier transform infra-red spectroscopy (FTIR)

FT-IR spectrum of the OMNP, Blank PLGA nanoparticles (particles lacking the magnetite and MTX), PLGA magnetite nanoparticles (particles loaded with magnetite but lacking MTX), MTX loaded PLGA nanoparticles (particles loaded with MTX but lacking magnetite) and MPNP are depicted in Fig. 3. Fe–O vibration at 590 cm^{-1}, carboxyl vibration at 1700-1800 cm^{-1} and hydroxyl vibration at 3200-3500 cm^{-1} are observed in these spectra.

3.3.5. Determination of MTX in MPNPs

MTX assay was performed using the validated calibration curve (y = 0.0164x - 0.0025 and r^2 0.9995) with acceptable precision and accuracy. The highest MTX-loaded particles in each modification steps chose, i.e. MPNP-28, MPNP-30, MPNP-32 and MPNP-35.

3.3.6. In vitro release of MTX

The release profile of MTX from the selected particles is shown in Fig. 4. The release profile of all the formulations best fitted the Higuchi model acquiring the highest r^2 value, comparatively.

3.3.7. In vitro cytotoxicity study

The cytotoxicity results of MTX, OMNPs, blank PLGA magnetic nanoparticles and selected MPNPs for 24, 48 and 72 h are shown in Fig. 5.

4. Discussion

Numerous studies have investigated the controlled delivery of a hydrophilic drug encapsulated into a hydrophobic carrier. However, efficient drug entrapment into the carrier of opposite nature has always been a challenge [18,23]. The easiest and highly used method for the incorporation of a hydrophilic drug in a hydrophobic carrier is the double emulsion solvent evaporation method [24,25].

There are different factors affecting the performance of every particulate system. Particle size is one of the important ones [19,26]. In

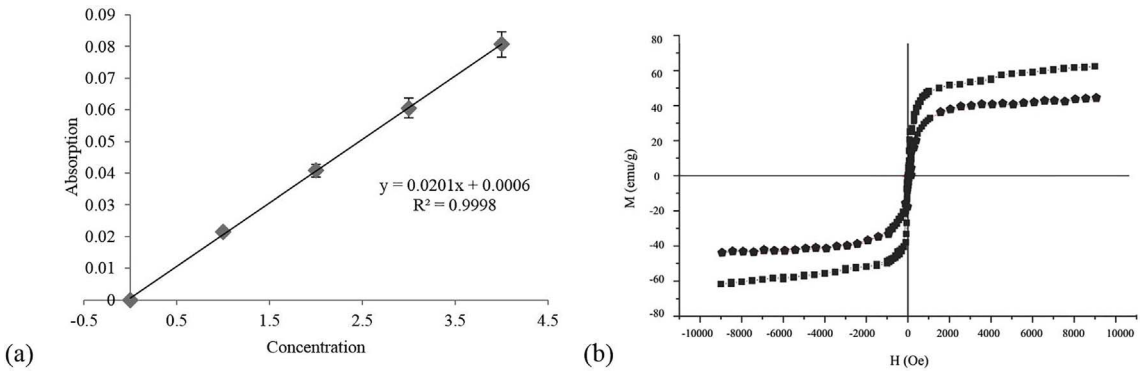

Fig. 2. (a) Standard curve of iron; (b) Magnetization curve of OMNPs (square line) and MPNP-35 (pentagon line). The data represent n = 3 trials.

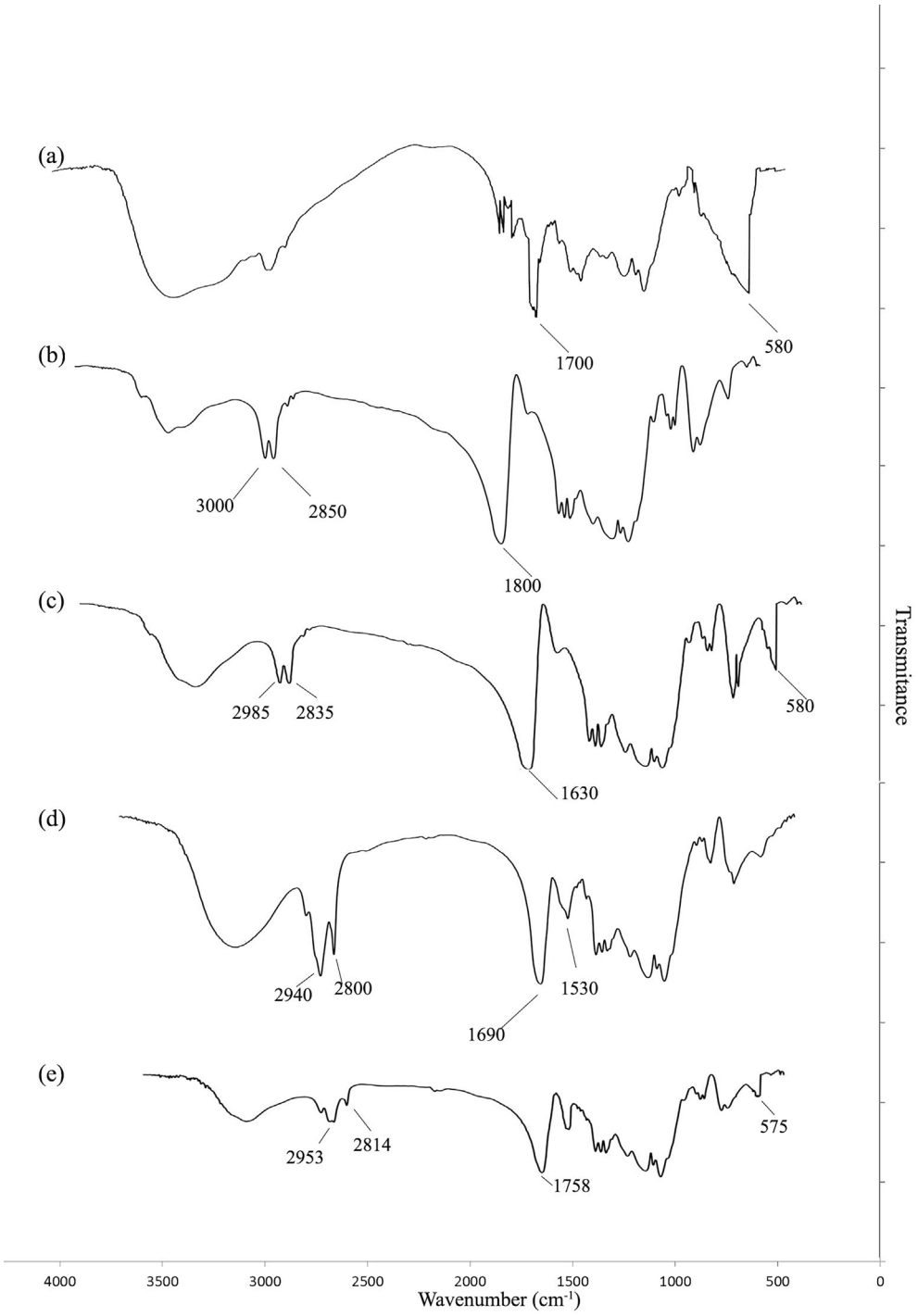

Fig. 3. FT-IR spectrum of (a) OMNP, (b) Blank PLGA nanoparticles, (c) PLGA magnetite nanoparticles, (d) MTX loaded PLGA nanoparticles, and (e) MPNP-35.

this study, a factorial design was performed in three levels to evaluate the size of the acquired particles. Among various effective parameters, drug to polymer ratio, PVA concentration (as surfactant) and solvent evaporation speed were selected. The resultant wide range of particle sizes is reported in Table 1.

Generally, increasing the polymer's viscosity led to enhanced resistance of organic phase droplets to shear stress, which, in turn, led to the formation of larger particles [27]. As predicted, larger particles were acquired as the amount of polymer increased (Table 1).

There are numerous reports discussing the effect of PVA concentration on particle size [28–30]. It has been reported that using PVA as surface-active stabilizer can produce smaller-sized particles with high entrapment efficiency and a sustained release profile [24]. However, increasing PVA would elevate the viscosity and the required shear force [31]. Considering our previous investigation, larger-sized particles were produced by 0.5% of PVA in comparison with 1% of PVA [21]. Hence, in this research, the investigated PVA concentrations were 1%–3%. The results showed that increasing PVA concentration produced larger particles. This may be due to insufficient mixing energy that is unable to overcome the provided force induced by the viscosity of the dissolved colloid stabilizer, PVA. As a result, heterogeneous droplets and broad size distribution were produced (Table 1).

It was reported that increasing the mixing force would raise shear stress, resulting not only in smaller-sized particles [29,32] but also

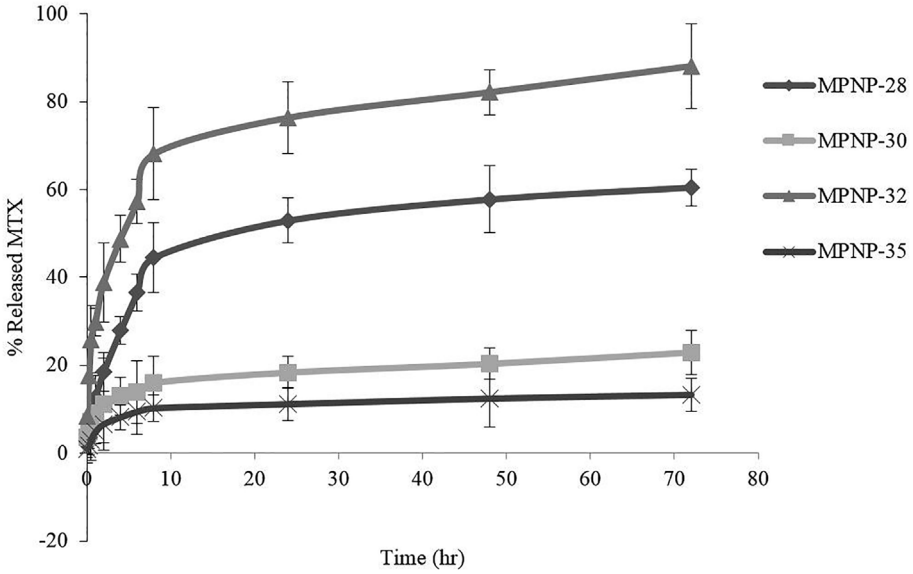

Fig. 4. Comparison of drug release from selected formulations.

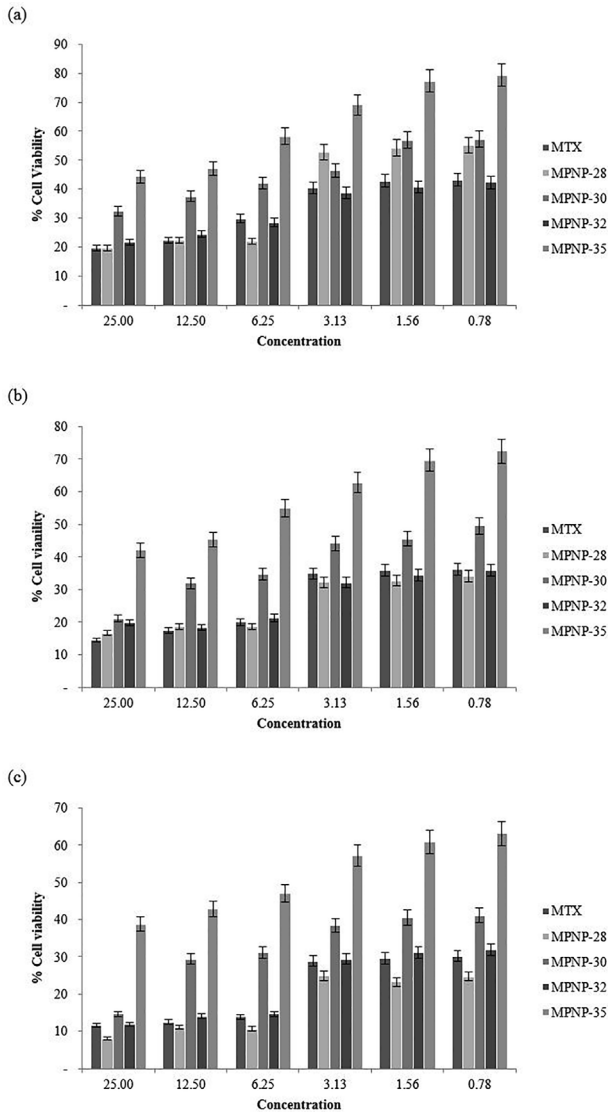

Fig. 5. Cytotoxicity evaluation of MTX, MPNP-28, MPNP-30, MPNP-32 and MPNP-35 in (a) 24hr., (b) 48hr., and (c) 72hr.

probably facilitating organic solvent evaporation from primary droplets and the rapid solidification of particles, which may reduce their size [29]. As expected, increasing the stirring speed from 750 to 1000 rpm produced smaller particles. Surprisingly, raising the stirring speed to 1400 rpm from 1000 rpm resulted in larger particles. This could be due to the effect of the stirrer's magnetic field that led to the aggregation of droplets and produced larger particles (Table 1). Altogether, the smallest particle size was achieved by a drug to polymer ratio of 1:1, a PVA concentration of 1%, and a stirring speed of 1000 rpm.

Encapsulation efficiency and drug loading depend on drug hydrophilicity and matrix materials [19]. Generally, previous literature reported high encapsulation efficiency for hydrophobic drugs in PLGA particles [22,33], which is attributed to greater drug solubility in the internal organic phase as compared to the external aqueous phase [26,34]. The hydrophilicity of MTX makes its encapsulation into hydrophobic carriers a bit challenging [19]. In this study, some assumingly effective parameters were investigated to increase the loading and encapsulation efficiency of MTX; these parameters included the amount of MTX, the effect of primary emulsion stabilization, and the effect of the external phase's pH, and the nature of the external phase components.

One of the important factors affecting loading parameters is the drug amount and its ratio to polymer [35]. As the volume fraction of the internal aqueous phase increased, the probability of the drug solution contacting with the external phase was enhanced, which could result in drug loss from primary emulsion and the lowering of encapsulation efficiency [30,31]. Taking our results into consideration, increasing the drug to polymer ratio from 1 to 2.5 resulted in elevating the encapsulation efficiency from 8.28 ± 3.7% to 16.87 ± 5.1%; meanwhile, raising the drug to polymer ratio to 5 resulted in decreasing the encapsulation efficiency to 13.07 ± 8.6%. This may be attributed to the inappropriate formation of primary emulsion. These data exhibit that a drug to polymer ratio of 2.5 can result in particles with higher encapsulation efficiency (Table 3).

The stabilization of primary emulsion (W_1/O) was reported as an effective parameter in improving the encapsulation of water-soluble drugs [19]. It was assumed that using a stabilizer (span®80, HLB of 4.8) may prevent distribution of MTX from the primary emulsion into the external aqueous phase. Accordingly, adding 2% stabilizer increased the encapsulation efficiency to 33.24 ± 2.2%. However, as the concentration of stabilizer was raised to 4%, the encapsulation efficiency was reduced to 27.87 ± 5.5%. The encapsulation efficiency improved when 2% stabilizer was used; however, it decreased with a higher concentration of stabilizer. This may be attributed to the rapid coating

of primary emulsion and reduction of time required for the formation of primary W_1/O emulsion with an adequate amount of MTX (Table 3).

Previous reports mentioned that drug solubility and distribution into the external phase would reduce by the external phase pH adjustment, which leads to increase MTX encapsulation efficiency [36]. Considering MTX cleavage from the particles in acidic conditions, and also the increased MTX solubility and distribution in the external phase at alkalized pH [31]; the effect of external phase pH on loading parameters was examined. The results showed that adjusting pH of the external phase to 5 increases the encapsulation efficiency of MTX up to 76.44 ± 2.91% (Table 3).

Previous studies have shown the effect of the rapid hardening of particles on drug loading parameters. It is shown that increasing the stirring speed may accelerate the hardening of particle; in such cases, rapidly hardened particles are laden with more drug amounts. This effect was also reported for the extraction phase content [30,31]. In this study, the encapsulation efficiency increased while using 1% paraffin in the extraction phase (Table 3). In this situation, the affinity of the hydrophilic drug for partitioning into the external phase decreased. As a result, the drug was not departed from particles during hardening and washing procedures. In the same manner, using PVA solution can increase the viscosity of the external phase and reduce its ability to dissolve the hydrophilic MTX. Therefore, the distribution of MTX in the external phase decreased and its encapsulation efficiency was elevated. However, using paraffin in the extraction phase increased the MTX encapsulation efficiency more than PVA.

Overall, the selected formulation was MPNP-35 with encapsulation efficiency and drug loading of 94.57 ± 2.06% and 18.91 ± 4.1%, respectively. The SEM image of polymeric particles MPNP-35 exhibited almost uni-dispersed particles with rough surfaces (Fig. 1).

The synthesis and characterization of oleic acid coated magnetite nanoparticles (OMNPs) were reported in our previous publication [4]. Herein, atomic absorption spectroscopy was reported to be an easy and reliable method to measure the iron content of polymeric particles [32,37]. A validated calibration curve in the range of 1–4 μg/ml of iron was obtained and used as reference (Fig. 2a). In previous studies, 65% [38], 70% [32] and 90% [30] magnetite encapsulation was reported. Magnetite encapsulation of more than 70% was reported to be suitable for magnetically guided systems due to the short time required for retention of particles [24]. Our results indicated a magnetite encapsulation of 84.31% for MPNP-35. It is worth mentioning that no systemic toxicity was expected with this encapsulation amount of iron oxide since the iron quantity of particles was much less than the amount used as contrast agents [8].

The magnetic saturation of particles depends on the amount of encapsulated magnetite, polymer type, particle size, and magnetite localization in particles. Coating magnetite with a magnetically dead layer of polymer reduces the primary magnetic saturation. A magnetization saturation of 14emu/g to 23.7emu/g has been reported for polymer coated particles [24]. In this study, particles with magnetic saturation of 43emu/g were achieved. This high saturation may be attributed to the high magnetic saturation of primary synthesized magnetite (72emu/g), their high loading (84.31%) and maybe their dispersion near the surface of particles. Neither remanence nor coercivity was observed in the magnetization curve, which exhibited superparamagnetic behavior in resultant particles (Fig. 2b).

The FTIR analysis (Fig. 3) showed the typical peaks of PLGA: 2850-3000 cm^{-1} (−CH, $-CH_2$, $-CH_3$), 1700-1800 cm^{-1} (–C = O), 1050-1250 cm^{-1} (C–O), and 3200-3500 cm^{-1} (−OH). In magnetite loaded particles, the observed Fe–O peak at 580-590 cm^{-1} and C = O peak at 1630 cm^{-1} indicated oleic acid coated magnetite is encapsulated with no specific interaction. The MTX loaded particles exhibited two characterizing peaks of MTX (1634 $cm^{-1}$and 1530 cm^{-1}). The other peaks were covered by PLGA peaks. In MPNPs; most of the absorption peaks from pure samples overlapped as no specific interaction occurred.

The MTX *in vitro* release from particles was investigated in previously reported PBS media [20,21]. As reported, the initial burst release of MTX from MPNP-28 can be related to the dispersion of MTX in the near surface layer of particles [35]. Using span® 80 as a primary emulsion stabilizer significantly decreased the burst release of MTX from particles (MPNP-30). This observation may be due to the lower amount of MTX, which can distribute into the superficial layers of particles. The very high burst release of MTX was observed from particles that were prepared in the external phase with pH of 5 (MPNP-32). This indicated that MTX was precipitated on the surface of the particles and released instantly. The burst release was almost eliminated from particles prepared in the external phase containing 1% paraffin (MPNP-35). This result implied the possible existence of a paraffin layer on the surface of particles that makes the distribution of MTX slower. Although the amount of MTX released from selected formulations varied significantly, all of them were best fitted to the Higuchi model that yielding the highest r^2 value comparatively.

The MTT test is widely used to evaluate the cytotoxicity of particles. Water soluble MTT can be reduced by metabolically active mitochondria in viable cells and form a water insoluble formazan product. The yellow color of MTT transforms to purple during this process [28]. It was reported that MTX should be incubated with cells in a concentration of about 1 μmol per liter for a minimum of 6 h in order to act [39].

The toxicity of particles can be attributed not only to the encapsulated drug but may also be due to the nature of the polymer and other components used for the preparation of particles [40]. The primary investigation indicated that neither the synthesized magnetite nor the blank particles were cytotoxic at investigated concentrations.

The cytotoxicity results of MPNP-28, MPNP-30, MPNP-32 and MPNP-35 formulations are shown in Fig. 5. The results were statistically compared and whenever the *p* value was less than 0.05, it was considered significantly different. The cytotoxicity of the MPNP-28 formulation was the same or a bit higher than MTX solution. The reported 40% burst release for this formulation could explain this result. Cell viability in contact with MPNP-30 formulation was higher than the MTX solution. Since drug release from these particles is only about 20% in 72 h, the obtained results were almost expected. No statistically significant difference was observed between the cytotoxicity of MPNP-32 formulation and the MTX solution. This can be attributed to the high burst release of the formulation (about 70%). Considering that the MPNP-35 formulation released about 10% of its encapsulated drug, its cell viability was higher than the MTX solution.

In general, the results have shown that the toxicity of particles is attributed to the amount and pattern of MTX release. It is possible to decide the suitable formulation regarding the desired therapeutic goal. Although the MPNP-28 and MPNP-32 formulations have almost the same toxicity as the MTX solution, these particles can be localized in the desired target site; they mostly affect malignant cells and reduce the side effects of MTX. The MPNP-30 and MPNP-35 formulations can be suitable for long term therapy, thus preventing repeated injections of MTX solution. However, they seemed to need the loading dose for a desirable effect. *In vivo* tests are essential for evaluating the effect of these formulations in detail.

5. Conclusion

Magnetically guided systems have shown remarkable benefits in biomedical fields. Hence, they were considered suitable for localized and regional drug delivery. Herein, with the aim of local MTX delivery, magnetite loaded PLGA nanoparticles were prepared and characterized. Polymeric carriers were prepared and optimized in respect of their particle size and loading parameters. Our study resulted in nanoparticles with suitable magnetic and drug loading properties, which showed similar cytotoxicity with the MTX solution on the breast cancerous cell line, SK-BR-3. Considering the localization of particles at the target site, the promising results in reducing the side effect of MTX, can be expectable. Despite promising benefits that may be offered by

magnetically guided systems, outstanding issues should be addressed and further *in vivo* investigations are crucial.

Declaration of interest

The authors report no declarations of interest.

Acknowledgments

Authors would like to acknowledge Dr. Nasrollah Erfani from Shiraz Institute of Cancer Research for his assistance in cytotoxicity studies.

Appendix A. Supplementary data

Supplementary data related to this article can be found at http://dx.doi.org/10.1016/j.jddst.2018.01.002.

References

[1] A. Malik, T.T. Butt, S. Zahid, F. Zahid, S. Waquar, M. Rasool, et al., Use of magnetic nanoparticles as targeted therapy: theranostic approach to treat and diagnose cancer, Journal of Nanotechnology 2017 (2017), https://doi.org/10.1155/2017/1098765.

[2] S. Alipour, H. Montaseri, A. Khalili, M. Tafaghodi, Non-invasive endotracheal delivery of paclitaxel-loaded alginate microparticles, J. Chemother. 28 (2016) 411–416, http://dx.doi.org/10.1080/1120009X.2015.1105624.

[3] J.H. Park, M. Ye, K. Park, Biodegradable polymers for microencapsulation of drugs, Molecules 10 (2005) 146–161, http://dx.doi.org/10.3390/10010146.

[4] H. Montaseri, S. Alipour, M.A. Vakilinezhad, Development, evaluation and optimization of superparamagnetite nanoparticles prepared by co-precipitation method, J. Res. Pharmaceut. Sci. 12 (2017) 274–282, http://dx.doi.org/10.4103/1735-5362.212044.

[5] M.F. Silva, A.A.W. Hechenleitner, J.M. Irache, A.J.A. Oliveira, E.A.G. Pineda, Study of thermal degradation of PLGA, PLGA nanospheres and plga/maghemite superparamagnetic nanospheres, Mater. Res. 18 (2015) 1400–1406, http://dx.doi.org/10.1590/1516-1439.045415.

[6] N.S. Barakat, Magnetically modulated nanosystems: a unique drug-delivery platform, Nanomedicine 4 (2009) 799–812, http://dx.doi.org/10.2217/nnm.09.66.

[7] V.V. Mody, A. Cox, S. Shah, A. Singh, W. Bevins, H. Parihar, Magnetic nanoparticle drug delivery systems for targeting tumor, Appl. Nanosci. 4 (2014) 385–392, http://dx.doi.org/10.1007/s13204-013-0216-y.

[8] A.H. Lu, E.L. Salabas, F. Schuth, Magnetic nanoparticles: synthesis, protection, functionalization, and application, Angew Chem Int 46 (2007) 1222–1244, http://dx.doi.org/10.1002/anie.200602866.

[9] J. Chomoucka, J. Drbohlavova, D. Huska, V. Adam, R. Kizek, J. Hubalek, Magnetic nanoparticles and targeted drug delivering, Pharmacol. Res. 62 (2010) 144–149, http://dx.doi.org/10.1016/j.phrs.2010.01.014.

[10] H. Yang, M. Hua, H. Liu, C. Huang, K. Wei, Potential of magnetic nanoparticles for targeted drug delivery, Nanotechnol. Sci. Appl. 5 (2012) 73–86, http://dx.doi.org/10.2147/NSA.S35506.

[11] K. Derakhshandeh, M. Soheili, S. Dadashzadeh, R. Saghiri, Preparation and in vitro characterization of 9-nitrocamptothecin-loaded long circulating nanoparticles for delivery in cancer patients, Int. J. Nanomed. 5 (2010) 463–471 PMCID: PMC2950404.

[12] R. Madhwi, P. Kumar, B. Kumar, Singh G. Sharma, O.P. Katare, et al., Vivo pharmacokinetic studies and intracellular delivery of methotrexate by means of Glycine-tethered plga-based polymeric micelles, Int. J. Pharm. (Amst.) 519 (2017) 138–144, http://dx.doi.org/10.1016/j.ijpharm.2017.01.021.

[13] X.Y. Li, H. Li, Y. Zhang, S. Gao, C.P. Dong, G.F. Wu, Development of albumin coupled, cholesterol stabilized, lipid nanoemulsion of methotrexate, and TNF-α inhibitor for improved in vivo efficacy against rheumatoid arthritis, AAPS PharmSciTech (2017), http://dx.doi.org/10.1208/s12249-017-0762-9.

[14] A. Jain, G. Sharma, V. Kushwah, N.K. Garg, P. Kesharwani, G. Ghoshal, et al., Methotrexate and beta-carotene loaded-lipid polymer hybrid nanoparticles: a preclinical study for breast cancer, Nanomedicine 15 (2017) 1851–1872, http://dx.doi.org/10.2217/nnm-2017-0011.

[15] M. Joshi, P. Kumar, R. Kumar, G. Sharma, B. Singh, O.P. Katare, et al., Aminated carbon-based "cargo vehicles" for improved delivery of methotrexate to breast cancer cells, Mater Sci Eng C Mater Biol Appl. 75 (2017) 1376–1388, http://dx.doi.org/10.1016/j.msec.2017.03.057.

[16] A.L. Boechat, C.P. Oliveira, A.M. Tarragô, A.G. Costa, A. Malheiro, S.S. Guterres, et al., Methotrexate-loaded lipid-core nanocapsules are highly effective in the control of inflammation in synovial cells and a chronic arthritis model, Int. J. Nanomed. 10 (2015) 6603–6614, http://dx.doi.org/10.2147/IJN.S85369.

[17] Q. Dang, C. Liu, Y. Wang, J. Yan, H. Wan, B. Fan, Characterization and biocompatibility of injectable microspheres-loaded hydrogel for methotrexate delivery, Carbohydr. Polym. 136 (2016) 516–526, http://dx.doi.org/10.1016/j.carbpol.2015.09.084.

[18] M.H. Lee, H.R. Lim, T.H. Lee, J.C. Park, Preparation of PLGA microparticles by a double emulsion solvent technique for sustained release of (-)-epigallocatechin gallate (EGCG) and their growth inhibitory effect on rat aortic smooth muscle cells, Biomater. Res. 13 (2009) 11–15 http://ir.ymlib.yonsei.ac.kr/handle/22282913/104715.

[19] A.L. Silva, R.A. Rosalia, A. Sazak, M.G. Carstens, F. Ossendorp, J. Oostendorp, et al., Optimization of encapsulation of a synthetic long peptide in PLGA nanoparticles: low-burst release is crucial for efficient CD8 + T cell activation, Eur. J. Pharm. Biopharm. 83 (2013) 338–345, http://dx.doi.org/10.1016/j.ejpb.2012.11.006.

[20] A. Singh, N. Thotakura, R. Kumar, B. Singh, G. Sharma, O.P. Katare, et al., PLGA-soya lecithin based micelles for enhanced delivery of methotrexate: cellular uptake, cytotoxic and pharmacokinetic evidences, Int. J. Biol. Macromol. 95 (2017) 750–756, http://dx.doi.org/10.1016/j.ijbiomac.2016.11.111.

[21] F. Ahmadi, H. Afrooz, F. Fallahzadeh, S.H. Mousavi-Fard, S. Alipour, Design and characterization of paclitaxel-verapamil co-encapsulated PLGA nanoparticles: potential system for overcoming P-glycoprotein mediated MDR, J. Drug Deliv. Sci. Technol. 41 (2017) 174–181, http://dx.doi.org/10.1016/j.jddst.2017.06.020.

[22] S. Alipour, H. Montaseri, M. Tafaghodi, Inhalable, large porous PLGA microparticles loaded with paclitaxel:preparation, in vitro and in vivo characterization, J. Microencapsul. 32 (2015) 661–668, http://dx.doi.org/10.3109/02652048.2014.944949.

[23] R. Dinarvand, N. Sepehri, S. Manoochehri, H. Rouhani, F. Atyabi, Polylactide-co-glycolide nanoparticles for controlled delivery of anticancer agents, Int. J. Nanomed. 6 (2011) 877–895, http://dx.doi.org/10.2147/IJN.S18905.

[24] M. Hamoudeh, A. Al Faraj, E. Canet-Soulas, F. Bessueille, D. Léonard, H. Fessi, Elaboration of PLLA-based superparamagnetic nanoparticles: characterization, magnetic behaviour study and in vitro relaxivity evaluation, Int. J. Pharm. (Amst.) 338 (2007) 248–257, http://dx.doi.org/10.1016/j.ijpharm.2007.01.023.

[25] C. Sun, C. Fang, Z. Stephen, O. Veiseh, S. Hansen, D. Lee, et al., Tumor-targeted drug delivery and MRI contrast enhancement by chlorotoxin-conjugated iron oxide nanoparticles, Nanomedicine 3 (2008) 495–505, http://dx.doi.org/10.2217/17435889.3.4.495.

[26] N. Butoescu, O. Jordan, E. Doelker, Intra-articular drug delivery systems for the treatment of rheumatic diseases: a review of the factors influencing their performance, Eur. J. Pharm. Biopharm. 73 (2009) 205–218, http://dx.doi.org/10.1016/j.ejpb.2009.06.009.

[27] A.S. Lübbe, C. Alexiou, C. Bergemann, Clinical applications of magnetic drug targeting, J. Surg. Res. 95 (2001) 200–206, http://dx.doi.org/10.1006/jsre.2000.6030.

[28] L.S. Liang, J. Jackson, W. Min, V. Risovic, K.M. Wasan, H.M. Burt, Methotrexate loaded poly(L-lactic acid) microspheres for intra-articular delivery of methotrexate to the joint, J. Pharmacol. Sci. 93 (2004) 943–956, http://dx.doi.org/10.1002/jps.20031.

[29] H. Zhao, J. Gagnon, U.O. Hafeli, Process and formulation variables in the preparation of injectable and biodegradable magnetic microspheres, Biomagn. Res. Technol. 5 (2007), http://dx.doi.org/10.1186/1477-044X-5-2 DOI: 10.1186/1477-044X-5-2.

[30] N. Butoescu, O. Jordan, A. Petri-Fink, H. Hofmann, E. Doelker, Co-encapsulation of dexamethasone 21-acetate and SPIONs into biodegradable polymeric microparticles designed for intra-articular delivery, J. Microencapsul. 25 (2008) 339–350, http://dx.doi.org/10.1080/02652040801999551.

[31] S. Freitas, H.P. Merkle, B. Gander, Microencapsulation by solvent extraction/evaporation: reviewing the state of the art of microsphere preparation process technology, J. Contr. Release 102 (2005) 313–332, http://dx.doi.org/10.1016/j.jconrel.2004.10.015.

[32] M. Hamoudeh, R. Diab, H. Fessi, C. Dumontet, D. Cuchet, Paclitaxel-loaded microparticles for intratumoral administration via the TMT technique: preparation, characterization, and preliminary antitumoral evaluation, Drug Dev. Ind. Pharm. 34 (2008) 698–707, http://dx.doi.org/10.1080/03639040701842444.

[33] R.Y. Hong, B. Feng, X. Cai, G. Liu, H.Z. Li, J. Ding, et al., Double-miniemulsion preparation of fe_3O_4/poly(methyl methacrylate) magnetic latex, J. Appl. Polym. Sci. 112 (2009) 89–98, http://dx.doi.org/10.1002/app.29403.

[34] R.M. Mainardes, M.P.D. Gremião, R.C. Evangelista, Thermoanalytical study of praziquantel-loaded PLGA nanoparticles, Rev. Bras. Ciênc. Farm 42 (2006) 523–530, http://dx.doi.org/10.1590/S1516-93322006000400007.

[35] S.K. Dey, B. Mandal, M. Bhowmik, L.K. Ghosh, Development and in vitro evaluation of Letrozole loaded biodegradable nanoparticles for breast cancer therapy, Braz. J. Pharm. Sci. 45 (2009) 585–591 https://doi.org/10.1590/S1984-82502009000300025.

[36] N. Kohler, C. Sun, J. Wang, M. Zhang, Methotrexate-Modified superparamagnetic nanoparticles and their intracellular uptake into human cancer cells, Langmuir 21 (2005) 8858–8864, http://dx.doi.org/10.1021/la0503451.

[37] S.S. Yu, R.L. Scherer, R.A. Ortega, C.S. Bell, C.P. O'Neil, J.A. Hubbell, et al., Enzymatic- and temperature-sensitive controlled release of ultrasmall superparamagnetic iron oxides (USPIOs), J. Nanobiotechnol. 9 (2011), http://dx.doi.org/10.1186/1477-3155-9-7 DOI: 10.1186/1477-3155-9-7.

[38] L. Ngaboni Okassa, H. Marchais, L. Douziech-Eyrolles, S. Cohen-Jonathan, M. Soucé, P. Dubois, et al., Development and characterization of sub-micron poly (d,l-lactide-co-glycolide) particles loaded with magnetite/maghemite nanoparticles, Int. J. Pharm. (Amst.) 302 (2005) 187–196 https://doi.org/10.1016/j.ijpharm.2005.06.024.

[39] A.M. Sieuwerts, J.G. Klijn, H.A. Peters, J.A. Foekens, The MTT tetrazolium salt assay scrutinized: how to use this assay reliably to measure metabolic activity of cell cultures in vitro for the assessment of growth characteristics, IC50-values and cell survival, Eur. J. Clin. Chem. Clin. Biochem. 33 (1995) 813–823 PMID: 8620058.

[40] M. Fleisher, Antifolate analogs: mechanism of action, analytical methodology, and clinical efficacy, Ther. Drug Monit. 15 (1993) 521–526 PMID: 8122287.